

1 **Root Responses to Heterogeneous Nitrate Availability are Mediated by *trans*-Zeatin in**
2 ***Arabidopsis* Shoots**

3
4
5 Arthur Poitout¹, Amandine Crabos¹, Ivan Petřík², Ondrej Novák², Gabriel Krouk¹, Benoît Lacombe¹ and
6 Sandrine Ruffel^{1*}

7
8
9
10 ¹Laboratoire de Biochimie et Physiologie Moléculaire des Plantes, UMR CNRS/INRA/Montpellier
11 SupAgro/UM, Institut de Biologie Intégrative des Plantes "Claude Grignon", 2 Place Viala, 34060
12 Montpellier, France; ²Laboratory of Growth Regulators, Centre of the Region Haná for Biotechnological
13 and Agricultural Research, Institute of Experimental Botany CAS and Faculty of Science of Palacký
14 University, CZ-78371 Olomouc, Czech Republic.

15
16 *Correspondence: Sandrine ruffel (sandrine.ruffel@inra.fr)
17

18 **ABSTRACT**

19

20 Plants are subjected to variable nitrogen (N) availability including frequent spatial nitrate (NO_3^-)
21 heterogeneity in soil. Thus, plants constantly adapt their genome expression and root physiology in order
22 to optimize N acquisition from this heterogeneous source. These adaptations rely on a complex and long-
23 distance root-shoot-root signaling network that is still largely unknown. Here, we used a combination of
24 reverse genetics, transcriptomic analysis, NO_3^- uptake experiments and hormone profiling under
25 conditions of homogeneous or heterogeneous NO_3^- availability to characterize the systemic signaling
26 involved. We demonstrate the important role of the *trans*-zeatin form of cytokinin (CK) in shoots, in
27 particular using a mutant altered for ABCG14-mediated *trans*-zeatin-translocation from the root to the
28 shoot, in mediating: (i) rapid long distance N-demand signaling and (ii) long term functional adaptations
29 to heterogeneous NO_3^- supply, including changes in NO_3^- transport capacity and root growth
30 modifications. We also provide insights into the potential CK-dependent and independent shoot-to-root
31 signals involved in root adaptation to heterogeneous N availability.

32 INTRODUCTION

33
34 Continuous functional and morphological plasticity of organs is one of the most fascinating differences
35 between plants and animals. Indeed, fixed in their environment, plants display a range of strategies
36 allowing them to face fluctuating resource availability. Plant roots are particularly implicated since they
37 are exposed to nutrient and water scarcity or over abundance. Signaling networks behind root adaptation
38 are now central targets for the new green revolution aiming at optimizing belowground functioning to the
39 benefit of aboveground development (Den Herder et al. 2010; Bishopp and Lynch 2015; Kong et al.
40 2014).

41 Consistent with the essential role of Nitrogen (N) for the biosynthesis of proteins, nucleic acids or
42 essential pigments such as chlorophyll, roots are responsive to the availability of this element (Gruber et
43 al. 2013; O'Brien et al. 2016; Kellermeier et al. 2014; Forde 2014). Responsiveness relies on the ability to
44 sense N availability. This sensing is commonly divided into 2 main branches: local perception of N in the
45 vicinity of the root (in particular the mineral N form nitrate, NO_3^-) and systemic perception of internal
46 N/NO_3^- availability at the whole organism level, relying on root-shoot-root signaling and integration of
47 information in different parts of the plant (Walch-Liu et al. 2005; Gansel et al. 2001; Li et al. 2014;
48 Alvarez et al. 2012). This dual sensing is integrated through an intricate signaling network permitting a
49 mutual control of root N acquisition with plant growth to ensure N homeostasis (Krouk et al. 2011).

50 In *Arabidopsis*, perception and propagation of local NO_3^- signaling has received a large attention.
51 The molecular actors involved in this process include the NO_3^- tranceptor NPF6.3/NRT1.1/CHL1 (Ho et
52 al. 2009; Krouk et al. 2010a), some kinases and phosphatase (CIPK8, CIPK23, ABI2, CPK10,30,32) (Hu
53 et al. 2009; Ho et al. 2009; Liu et al. 2017; L eran et al. 2015) and several transcription factors (NLP6/7,
54 TGA1/4, NRG2, SPL9) (Castaings et al. 2009; Marchive et al. 2013; Konishi and Yanagisawa 2013;
55 Alvarez et al. 2014; Xu et al. 2016; Krouk et al. 2010b) targeting the expression of genes involved in NO_3^-
56 transport and assimilation, also known as the Primary Nitrate Response (PNR) (Medici and Krouk 2014).
57 In addition, Ca^{2+} has been defined as a secondary messenger in this process (Riveras et al. 2015; Liu et al.
58 2017; Krouk 2017). Control of the N-response can be extended to additional transcription factors such as
59 ANR1, ARF8 and NAC4 or CLE peptides that are involved in N-dependent root development (Zhang and
60 Forde 1998; Vidal et al. 2013; Araya et al. 2014; Gifford et al. 2008) or bZIP1, LBD37/38/39 and BT2
61 transcription factors that control N-use (Rubin et al. 2009; Araus et al. 2016; Gutierrez et al. 2008). The
62 TCP20 transcription factor, which is not involved in PNR *per se*, physically interacts with NLP6/7 to
63 likely regulate the expression of NO_3^- -responsive genes and a cell cycle marker gene (Guan et al. 2014;
64 Guan et al. 2017; Li et al. 2005). Interestingly, TCP20 is also a regulator of root foraging in heterogeneous

65 N supply conditions (Guan et al. 2014) and thus could provide an anchorage point to understand how local
66 and systemic N-regulation is integrated (Guan et al. 2017).

67 However, the functioning of a signaling cascade upstream of these local regulators of root
68 physiology or morphology in response to the global N availability is poorly understood. This lack of
69 knowledge is probably due to the necessity to use complex experimental approaches such as split-root
70 system to address specifically the question of long distance signaling. Indeed, split-root experiments
71 provide a relevant framework to untangle the different local and systemic signaling occurring in plants.
72 The overall concept is to compare roots experiencing similar local hydro-mineral conditions but different
73 distant (other part of the root) media (Li et al. 2014). By comparing roots in the same local condition, any
74 differences between these roots can only be due to the impact of the long distance signal(s) (Figure 1A).
75 This system helped to define the landscape of the N related systemic signaling response and defined at
76 least 2 co-existing systemic signaling pathways (Ruffel et al. 2011; Li et al. 2014). The "N-demand" long
77 distance signal conveys the information that the whole plant is experiencing a distal N-deprivation, while
78 the "N-supply" signal conveys the information that some N has been found by the plant (Ruffel et al.
79 2011) (Figure 1A). Two components were identified in these signaling pathways: the role of C-terminally
80 encoded peptides (CEP) (Tabata et al. 2014) and cytokinins (CK) biosynthesis (Ruffel et al. 2011; Ruffel
81 et al. 2016).

82 The role of CEPs was recently demonstrated. Upon N-deprivation, CEPs are translocated to the
83 shoots where they are recognized by the CEP Receptor 1 kinase (Tabata et al. 2014). Within the shoot
84 vascular system, this recognition leads to the expression of small polypeptides that translocate toward the
85 roots and participate, in combination with local NO_3^- , in controlling specifically the transcript
86 accumulation of the main root high affinity NO_3^- transporter *NRT2.1* (Ohkubo et al. 2017; Ruffel and
87 Gojon 2017). However, in heterogeneous NO_3^- supply conditions, roots display a wide range of adaptive
88 responses including: the transcriptional regulation of hundred of genes, an enhanced lateral root
89 development, and an enhanced N acquisition (Gansel et al. 2001; Remans et al. 2006; Ruffel et al. 2008;
90 Ruffel et al. 2011; Mounier et al. 2014). The role of the CEP-derived long-distance signal remains to be
91 demonstrated in these other aspects of the adaptive response to N heterogeneity.

92 It has been shown that CKs are synthesized in roots and translocated to the shoots in response to N
93 provision, leading to the control of shoot growth (Takei et al. 2001; Takei et al. 2004; Sakakibara et al.
94 2006; Osugi et al. 2017). The crucial role of CK in root response to long distance signals was
95 demonstrated (Ruffel et al. 2011). However, an important question remains concerning the role of CK in
96 the shoots to actually trigger the root response in a systemic context. In other words, is active CK in the
97 shoots a component of the long-distance signaling controlling at the same time molecular and
98 physiological root response to NO_3^- heterogeneity?

99 In this work, we demonstrate that shoot *trans*-zeatin (*tZ*) type CK is indeed an essential element of
100 long-distance signaling that controls (i) transcriptional reprogramming of roots and shoots, (ii) root growth
101 and (iii) NO₃⁻ transport activity, in response to heterogeneous NO₃⁻ conditions. By combining a genetic
102 approach targeting modification of CK content and translocation with exhaustive measurements of CK
103 forms and a shoot transcriptome analysis, we demonstrate that unbalanced root response to NO₃⁻ provision
104 relies on the integration in shoots of *tZ*.

105
106 **RESULTS**
107
108 **Root to shoot cytokinin translocation controls transcriptional response to N-demand long distance**
109 **signal**
110

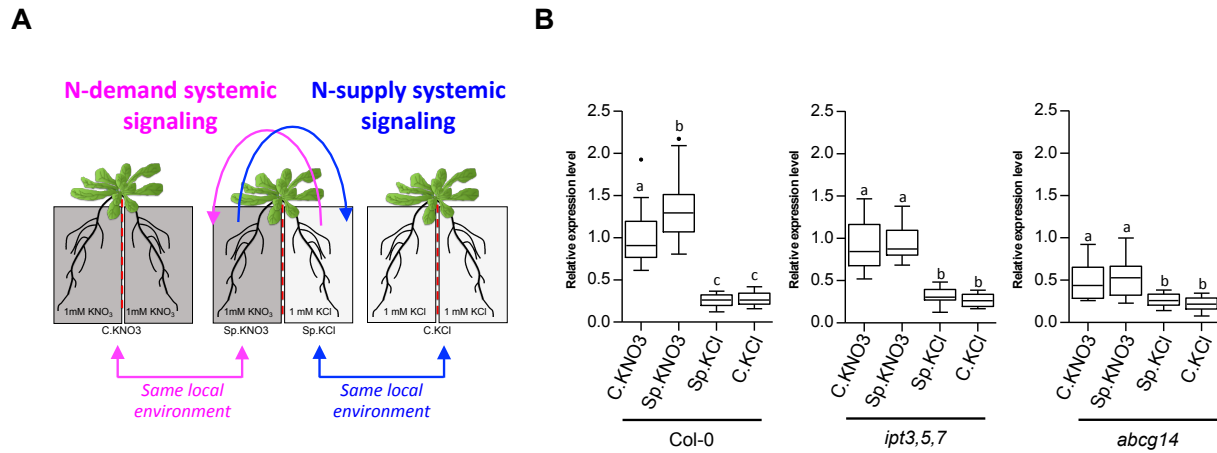
111 To investigate the role of CK root to shoot translocation in N-related systemic signaling, we characterized
112 a mutant lacking the ABCG14 (ATP-Binding Cassette Transporter Subfamily G) transporter and thus
113 impaired in delivering CK to the shoot (Ko et al. 2014; Zhang et al. 2014). To do so, wild-type (WT) and
114 mutant plants were grown in a hydroponic split-root system. Our experimental framework consisted in 3
115 conditions of N provision, providing 4 different root samples (Figure 1A): (i) a homogeneous N-replete
116 environment (C.KNO₃: both compartments have 1 mM KNO₃), (ii) a homogeneous N-deprived
117 environment (C.KCl: both compartments have 1 mM KCl), and (iii) a heterogeneous split environment
118 (Sp.KNO₃/Sp.KCl: one compartment has 1 mM KNO₃, and the other has 1 mM KCl). Any difference
119 recorded between C.KNO₃ and Sp.KNO₃ samples is the signature of a N-demand long distance signal,
120 while any difference recorded between Sp.KCl and C.KCl samples is the signature of a N-supply long-
121 distance signal. This logic is applied throughout the whole manuscript (Figure 1A). This framework has
122 been used to test the specific and quick response of sentinel genes to N-systemic signaling that were
123 identified previously from a dynamical root transcriptomic analysis following plant transfer to
124 homogeneous or heterogeneous conditions (Ruffel et al. 2011). Sentinel genes belong to important
125 functions including the NO₃⁻ assimilation pathway (*NiR*, *G6PD3*, *UPMI*, *FNR2*) and NO₃⁻ transport
126 systems (*NRT2.1* (Filleur et al. 2001) and its functional partner *NRT3.1/NAR2.1* (Yong et al. 2010)).

127 In WT plants, mRNA accumulation of the sentinel genes in Sp.KNO₃ roots was higher compared to
128 the homogeneous control condition C.KNO₃, showing that Col-0 roots responded to NO₃⁻ heterogeneous
129 availability through a systemic N-demand signal (Figure 1B) (Ruffel et al. 2011). As expected, in these
130 hydroponic split-root conditions, the isopentenyltransferase *ipt3,5,7* mutant, altered for CK biosynthesis
131 (Miyawaki et al. 2006), displayed an alteration of the response to systemic N-demand (Figure 1B) (Ruffel
132 et al. 2011). In the *abcg14* mutant, the expression level of sentinel genes was lower as compared to Col-0,

133 but more importantly Sp.KNO3 roots did not display any significant stimulation of sentinel gene
134 expression as compared to C.KNO3 control roots. This demonstrates that *abcg14* is also impaired in
135 triggering the response to systemic N-demand signaling (Figure 1B). Therefore, CK root to shoot
136 translocation could be essential for plant response to heterogeneous environment. It is noteworthy that for
137 both mutants the expression level of sentinel genes is still responsive to the local NO_3^- availability
138 (C.KNO3 and Sp.KNO3 *versus* Sp.KCl, C.KCl; Figure 1B), showing that these mutants still preserve their
139 ability to detect NO_3^- *per se*.

140

141



142

143 **Figure 1. Perturbation of CK root to shoot translocation impairs the expression of N-demand sentinel genes.**

144 (A) WT and mutant plants were grown in hydroponic split-root conditions to decipher N-demand and N-supply
145 signaling.

146 (B) Relative expression level of sentinel genes was measured from roots harvested 6h30 after transfer in C.KNO₃,
147 Sp.KNO₃/Sp.KCl and C.KCl conditions in Col-0, *ipt3,5,7* and *abcg14*. Boxplots display the expression values of the
148 6 N-demand sentinel genes *NRT2.1*, *NRT3.1*, *NiR*, *G6PD3*, *UPMI* and *FNR2*. Individual expression values have
149 been normalized by the mean of the WT C.KNO₃ expression across all experiments. Values are the means (+/- SE)
150 of 3 independent experiments consisted each of 2 biological replicates corresponding to a pool of 3 plants. Different
151 letters indicate significant difference according to one-way analysis of variance followed by a Tukey post-hoc test,
152 $p < 0.05$.

153

154

155

156 **Active *trans*-zeatin in shoots controls the root response to systemic N-demand**

157
158 To determine how CK partitioning/homeostasis control the root specific reprogramming response to
159 heterogeneous NO₃⁻ supply, levels of the four basic isoprenoid CK types (*tZ*, isopentenyladenine iP, *cis*-
160 zeatin *cZ* and dihydrozeatin DHZ) and their derivatives (ribotides, ribosides, *O*-glucosides and *N*-
161 glucosides) were measured in roots and shoots, at the time point used to evaluate the response of sentinel
162 genes (Figure 1).

163

164 **CK partitioning is under the control of a combined effect of Nitrogen, IPTs and ABCG14.**

165

166 Firstly, as a control of our experimental system, we did a global analysis showing that the pattern of
167 accumulation of the 4 CK types is indeed impacted by the *ipt3,5,7* and *abcg14* mutations as expected (Ko
168 et al. 2014; Miyawaki et al. 2006) (Figure 2A). Moreover, we also provide insight into the response of CK
169 accumulation to NO₃⁻ provision in WT and these mutant genotypes (comparison C.KNO₃ *versus* C.KCl;
170 Figure 2A). As expected, the triple mutation in *IPT* genes led to a drastic decrease of *tZ* and iP-types in
171 both shoots and roots (Figure 2A). In accordance with the predominant role of *IPT3* and *IPT5* in NO₃⁻-
172 dependent CK biosynthesis (Takei et al. 2004), NO₃⁻ provision does not impact the low accumulation of *tZ*
173 and iP-types still synthesized in the *ipt3,5,7* mutant (Figure 2A). Contrary to what has been previously
174 observed, we did not see an increase of global *cZ*-type accumulation in the *ipt3,5,7* mutant (Miyawaki et
175 al. 2006) but rather a significant decrease in the roots (Figure 2A). Interestingly, an increase of global *cZ*-
176 type accumulation was rather observed in *abcg14* shoots in response to N-deprivation (C.KCl) (Figure
177 2A). A more detailed analysis of *cZ*-types revealed that in fact only *O*-glucosylated forms of *cZ* were
178 increased in *ipt3,5,7* in all conditions (Supplemental Figure 1, blue arrows) whereas in *abcg14* *O*-
179 glucosides as well as transported and active *cZ*-forms were increased in shoots as soon as N provision was
180 limited (Supplemental Figure 1, red arrows). Altogether, these results demonstrate that *cZ*-type
181 homeostasis is indeed modified when MEP pathway-dependent CKs are perturbed. In addition, our
182 experimental set-up provides an interesting framework to investigate the role of *cZ*-forms to maintain in
183 shoots a minimal CK activity required to respond to abiotic stress (Schafer et al. 2015).

184 For the *abcg14* mutation, perturbations of CK partitioning and accumulation were consistent with
185 previous data (Zhang et al. 2014; Ko et al. 2014). We indeed observed an increase in the accumulation of
186 *tZ*-, iP- and DHZ-types in roots and a decrease in the accumulation of *tZ*-types in shoots, in accordance
187 with the role of ABCG14 in root to shoot CK translocation (Figure 2A). Moreover, iP accumulation in the
188 *abcg14* mutant is increased by N provision (Supplemental Figure 2, green arrows). Very interestingly,
189 shoot iP content of the WT plants follows the level of root N provision and this aspect is very strongly

190 affected by the *abcg14* mutation (Supplemental Figure 1, pink arrows). In more detail, this resulted in a
191 lower accumulation of active iP-forms in C.KNO3 and a higher accumulation of all iP-forms in C.KCl in
192 the *abcg14* mutant (Supplemental Figure 1, pink arrows). Therefore, taken together, these results
193 demonstrate that the dynamic accumulation of *tZ* in shoots is under the control of the ABCG14 protein,
194 and that this differential accumulation also controls N-responsive accumulation of iP-type CKs.

195

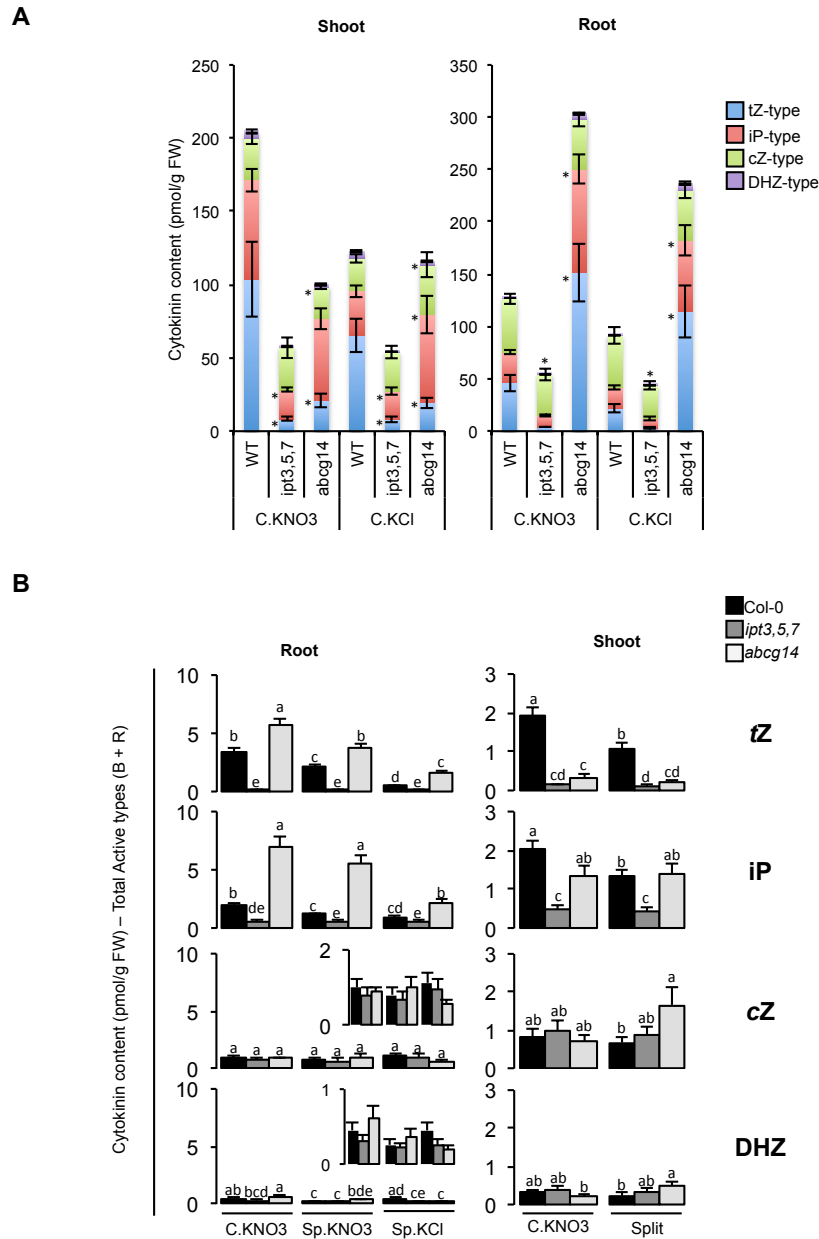
196 **Shoot and not root *tZ* accumulation explains root sentinel gene expression.**

197

198 To explain the early response of sentinel genes to the systemic N-demand signaling and their
199 perturbations in the mutant backgrounds (Figure 1B), we analyzed the accumulation of active and
200 transported CK-forms (Base and Riboside) in roots and shoots in the split-root framework (Figure 1A). No
201 obvious correlation was detected between gene expression (Figure 1B) and active-CK forms accumulation
202 in roots (Figure 2B, left panel). Indeed, the *ipt3,5,7* and *abcg14* mutants display an opposite phenotype
203 concerning *tZ* and iP accumulation whereas, in the same conditions, they both display the same gene
204 expression profile (loss of N-demand signaling). We thus conclude that CK accumulation in roots cannot
205 explain sentinel gene expression. However, shoot *tZ* accumulation can explain the root transcriptomic
206 profile. Indeed, we observed that shoot *tZ* accumulation is decreased by both the *ipt3,5,7* and *abcg14*
207 mutations (Figure 2B, right panel). In conclusion, the analysis of *ipt3,5,7* and *abcg14* mutants
208 demonstrates that *tZ* accumulation in shoots is an explanatory factor of root gene expression in response to
209 long-distance signaling.

210 Moreover, it is noteworthy that root *tZ* and iP differential accumulation between C.KNO3
211 Sp.KNO3 conditions are conserved in WT and the *abcg14* mutant (Figure 2B, left panel). This indicates a
212 control of root CK accumulation by a systemic CK-independent N-demand signaling. This is consistent
213 with our previous observations made on lateral root elongation harboring CK dependent and independent
214 branches (Ruffel et al. 2016).

215



216
 217 **Figure 2. Root and shoot CK-types accumulation points on the role of *tZ* accumulation in shoots.**
 218 (A) Stacked bar graphs display total CK accumulation and distribution of *tZ*, *iP*, *cZ* and DHZ type CK content in the
 219 shoots (left graph) and in the roots (right graph) from WT and mutant plants exposed to homogeneous C.KNO₃ or
 220 C.KCl conditions. Asterisks indicate significant differences of accumulation between mutants and Col-0, according
 221 to a Student Test, $p < 0.05$. If above the bar, the asterisk indicates that the accumulation of the 4 CK-types is different.
 222 (B) Barplots show active and transported (Base and Riboside) CK content (*tZ*, *iP*, *cZ* and DHZ) in the roots (left
 223 graphs) and in the shoots (right graphs) of WT and mutant plants in C.KNO₃ or split conditions. Values are the
 224 means (+/- SE) of 5 to 6 biological replicates collected from 4 independent experiments. Letters indicate significant
 225 differences between treated genotypes. *iP*: N^6 -(Δ^2 -isopentyl)adenine; *tZ*: *trans*-Zeatin; *cZ*: *cis*-Zeatin; DHZ: Dihydro-
 226 zeatin.

227 **Shoot genetic reprogramming in response to heterogeneous NO₃⁻ supply is perturbed in cytokinin**
228 **biosynthesis and translocation mutants.**

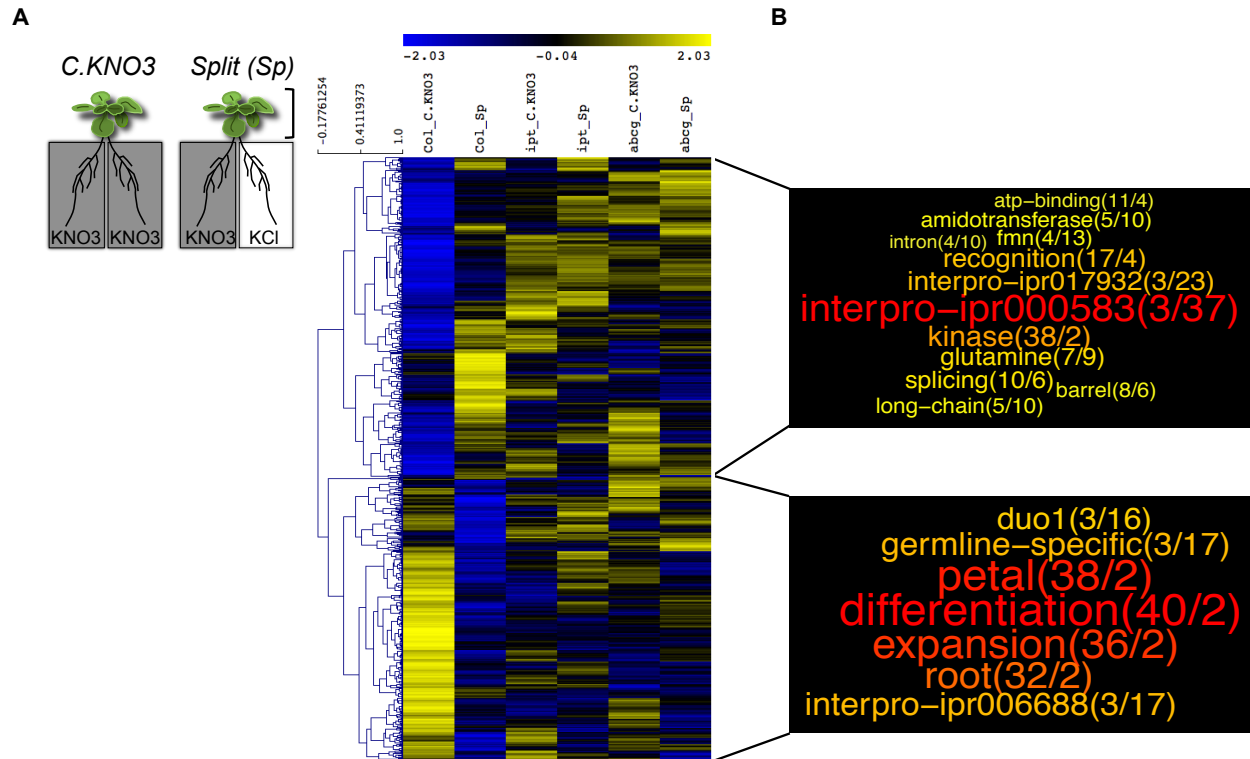
229
230 As we previously demonstrated that *tZ* accumulation in shoots is crucial to explain root sentinel adaptation
231 to long distance N-demand signaling, we decided to evaluate the impact of *ipt3,5,7* and *abcg14* mutations
232 on the response of the shoot transcriptome in plants experiencing homogeneous or heterogeneous NO₃⁻
233 supply (Figure 3A). To do so, *Arabidopsis* Gene1.1 ST Affymetrix array strips have been used (See
234 Material and Methods for details on samples, arrays and data analysis). In the WT, 780 transcript clusters
235 (probes equivalent) were significantly differentially accumulated between C.KNO3 and Split conditions.
236 422 were found to be up-regulated in Split conditions compared to the control C.KNO3 and 358 were
237 regulated in the opposite direction (Supplemental Table 1). Only the 745 non-ambiguous AGIs were kept
238 for the following analysis. Hierarchical clustering of their expression level in the 2 treatments (C.KNO3,
239 Split) and the 3 genotypes revealed that the regulation in Col-0 by heterogeneous NO₃⁻-provision was
240 strongly affected in the 2 mutants (Figure 3A). Therefore, in addition to being impaired in *tZ*
241 accumulation in response to N-supply, the 2 mutants undergo a perturbation of their capacity to reprogram
242 gene expression in response to NO₃⁻-supply, likely disrupting N-systemic signaling controlling root
243 responses. Interestingly, some semantic terms were enriched within the annotation of these genes,
244 indicating biological functions likely under the control of CK accumulation in shoots. Among the genes
245 up-regulated in heterogeneous compared to homogeneous NO₃⁻ condition, we found a significant
246 enrichment of 2 interpro domains, 'ipr000583' and 'ipr017932', which both correspond to glutamine
247 amidotransferase class-II domain found in 3 genes involved in glutamate synthesis (*i.e.*, AT2G41220,
248 AT3G24090, AT5G04140) (Figure 3B). Moreover, the overrepresentation of the 'glutamine' term was also
249 found in 4 other genes annotated as glutamine amidotransferase class-I and glutamate-ammonia ligase
250 (*i.e.*, AT1G53280, AT3G53180, AT4G26900, AT4G30550) (Figure 3B). This result suggests that, even if
251 NO₃⁻ is the genuine signal to trigger N-demand systemic signaling (Ruffel et al. 2011), its heterogeneous
252 supply triggers modification of an N assimilation pathway in shoots, in a CK-dependent manner.
253 Similarly, we observed term enrichment among the genes down-regulated in heterogeneous compared to
254 homogeneous NO₃⁻ conditions, corresponding to the interpro domain 'ipr006688' found in 3 ADP-
255 ribosylation factors (*i.e.*, AT3G49860, AT5G14670, AT1G02440) and 'duo1' (or 'germline-specific')
256 found in 2 genes annotated as C2H2 Zinc Finger proteins and HAPLESS 2 gene (*i.e.*, AT4G35280,
257 AT4G35700, AT4G11720) (Figure 3B).

258 By integrating the expression level of the whole genome data set (*i.e.*, 3 genotypes and 2
259 treatments), we also identified 669 unique genes responding similarly to the NO₃⁻ treatment in the shoots
260 of the 3 genotypes (Supplemental Table 2). This corresponds to genes whose regulation is likely not

261 related to CK-dependent long-distance signaling. Hierarchical clustering displayed a first level of
262 classification based on the differential regulation in NO_3^- heterogeneous versus homogeneous conditions
263 (Supplemental Figure 3A). The semantic enrichment analysis, of those genes revealed only few
264 meaningful terms, including, for example, the enriched terms 'uba-like' found in the annotation of 3 genes
265 related to ubiquitination processes (*i.e.*, AT2G17190, AT4G11740, AT5G50870) (Supplemental Figure
266 3B).

267 Altogether, this shoot transcriptomic analysis showed a massive and quick reprogramming of gene
268 expression accompanying distinct *tZ* accumulation in response to NO_3^- -supply. Moreover, this allowed us
269 to confirm the occurrence of CK-dependent and CK-independent branches of N systemic signaling (Ruffel
270 et al. 2016) and to narrow down the biological pathways associated with the respective signals.

271



272
 273 **Figure 3. CK-dependent shoot transcriptome changes in response to root heterogeneous NO₃⁻ supply.**
 274 (A) Shoots of Col-0, *ipt3,5,7* and *abcg14* plants transferred for 24 hrs in NO₃⁻ homogeneous (C.KNO3) or
 275 heterogeneous (Split) environment were harvested for transcriptomic analysis. Samples of 4 biological replicates
 276 from 4 independent experiments were used to perform the microarray analysis, using Arabidopsis Gene1.1 ST array
 277 Strip (Affymetrix GeneAtlas™). Hierarchical clustering of the 745 genes identified as differentially expressed in
 278 C.KNO3 versus Split conditions in the WT was performed with Multiple Experiment Viewer (MeV) software
 279 (<http://mev.tm4.org/>), using gene expression levels in the WT and the mutants.
 280 (B) Semantic enrichment in annotation of genes induced (at the top) or repressed (bottom) in Split condition
 281 compared to C.KNO3 in WT shoots, based on a GeneCloud analysis (<https://m2sb.org>). Beside each term, the first
 282 number corresponds to the number of genes containing the term and the second number gives the fold enrichment.
 283

284 ***ipt3,5,7* and *abcg14* mutations affect integrated root traits in response to heterogeneous NO_3^- supply.**

285
286 At a molecular level, sentinel genes responding specifically and quickly to a CK-dependent N-demand
287 systemic signaling are largely involved in NO_3^- transport and assimilation (e.g. NO_3^- transporter NRT2.1
288 or Nitrite Reductase) (Figure 1B). Therefore, we asked to what extent genetic perturbation of CK
289 biosynthesis and root to shoot translocation could affect the associated long-term adaptation of root
290 physiology to different N supply: root NO_3^- influx capacity and biomass (e.g. root dry weight). We also
291 decided to highlight the relationship between these two components of N acquisition. To do so we
292 combined root traits on single graphs allowing us to take into account the variability of plant growth
293 between independent biological replicates (Figure 4A).

294 In WT, both components (root dry mass and NO_3^- transport) responded significantly to N-systemic
295 signaling (N-demand and N-supply) since the mean values are significantly higher in Sp.KNO3 (5.8 mg
296 and $92 \mu\text{mol N.h}^{-1}.\text{g}^{-1}$ root DW) compared to C.KNO3 (3.6 mg and $56 \mu\text{mol N.h}^{-1}.\text{g}^{-1}$ root DW) and higher
297 in C.KCl (4.3 mg and $74 \mu\text{mol N.h}^{-1}.\text{g}^{-1}$ root DW) compared to Sp.KCl (2.9 mg and $28 \mu\text{mol N.h}^{-1}.\text{g}^{-1}$ root
298 DW) (Figure 4A, graphs on top). More importantly, this analysis revealed the existence of a relationship
299 between the two adaptive processes in NO_3^- supply roots (i.e. transport and biomass). Indeed, we observed
300 that WT plants having a strong developmental response display a lower NO_3^- transport adaptation and
301 *vice-versa* (Figure 4A, top left).

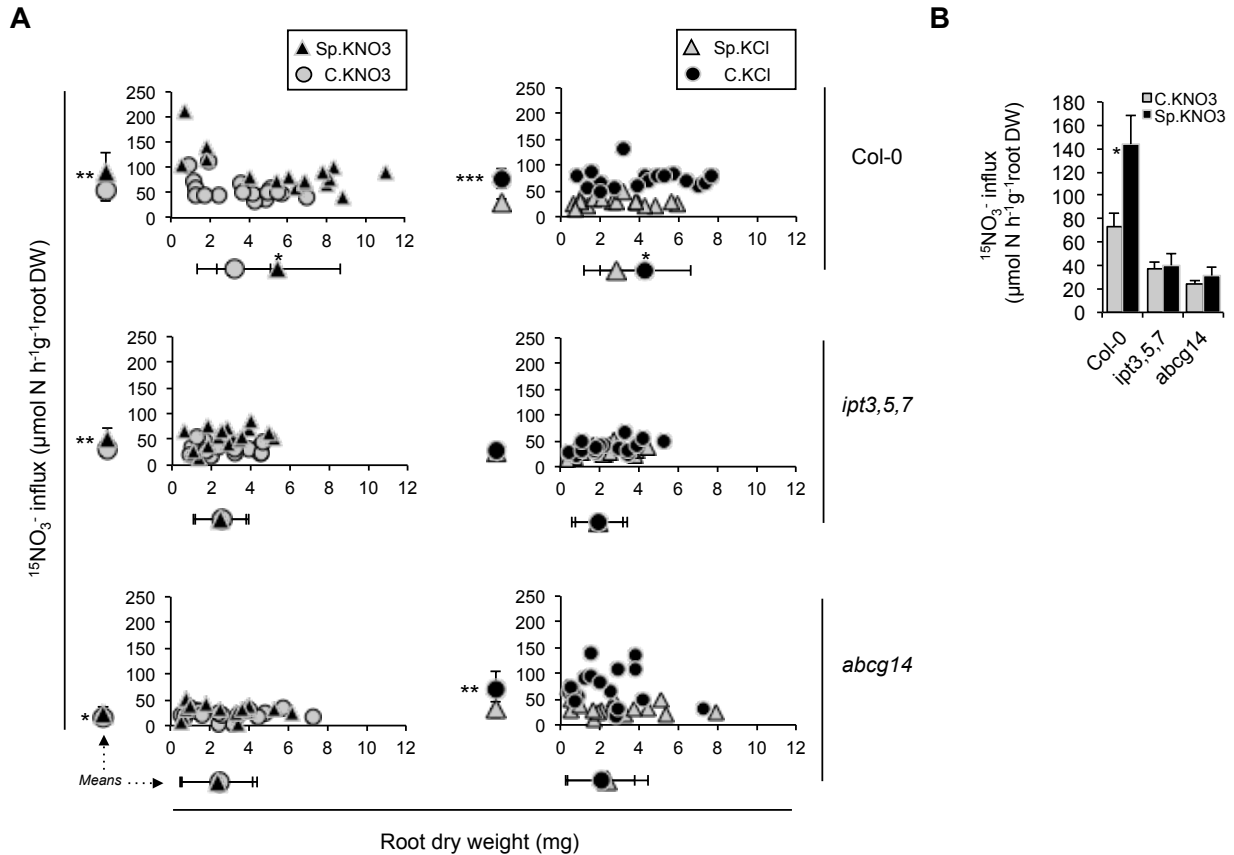
302 In the mutants, root biomass and NO_3^- influx responses to N-demand systemic signaling were
303 deeply perturbed (Figure 4A, left panel), suggesting that CK and more precisely root to shoot translocation
304 is a limiting factor for root response to a heterogeneous environment. The stimulation of root biomass
305 production in Sp.KNO3 compared to C.KNO3 was abolished (Figure 4A, left panel). According to the
306 strategy of WT plants described above, one would expect that the smallest root systems would display a
307 greater increase in NO_3^- influx as an alternative strategy to compensate for distal N-deprivation. Thus, the
308 mutants might compensate for their root biomass phenotype by increasing their NO_3^- transport activity.
309 However, this is not what we observed. Indeed, if we consider for instance only roots with a dry biomass
310 below the arbitrary value of 2 mg (expected to be the one to adapt the most their NO_3^- transport), WT
311 Sp.KNO3 roots displayed a NO_3^- influx significantly 2 times greater than their respective controls whereas
312 mutant Sp.KNO3 and C.KNO3 roots display the same low level of NO_3^- influx (Figure 4B). Therefore,
313 CK appears to be central to set up the two intertwined adaptive responses to heterogeneous NO_3^- supply
314 (i.e. NO_3^- transport and root development).

315 Interestingly, the two mutants did not behave similarly in response to the N-supply systemic
316 signaling (Figure 4A, right panel). Whereas CK biosynthesis is required to stimulate root proliferation and
317 NO_3^- influx when N is completely absent from the medium (Figure 4A, graph on middle right), the *abcg14*

318 mutant still maintained a NO_3^- influx capacity similar to Col-0 (*i.e.* 71 and 74 $\mu\text{mol N}\cdot\text{h}^{-1}\cdot\text{g}^{-1}$ root,
319 respectively) albeit the *abcg14* mutant displayed a higher variability than WT (Figure 4A, graphs on top
320 and bottom right).

321 Altogether, our results show that CKs have a broad role in regulating integrated adaptive traits in
322 response to long-distance signaling pathways. In the same way, the modulation of an even more
323 integrative trait controlled by N provision, that is the shoot/root ratio, is lost upon CK perturbation
324 (Supplemental Figure 4).

325 We conclude that CKs are deeply involved in the control of long-term plant adaptation to NO_3^-
326 heterogeneity and that CK-translocation cannot explain the entirety of these responses since it's likely not
327 the root to shoot *tZ* translocation that is involved in regulating root NO_3^- uptake capacity by N-supply
328 systemic signaling.



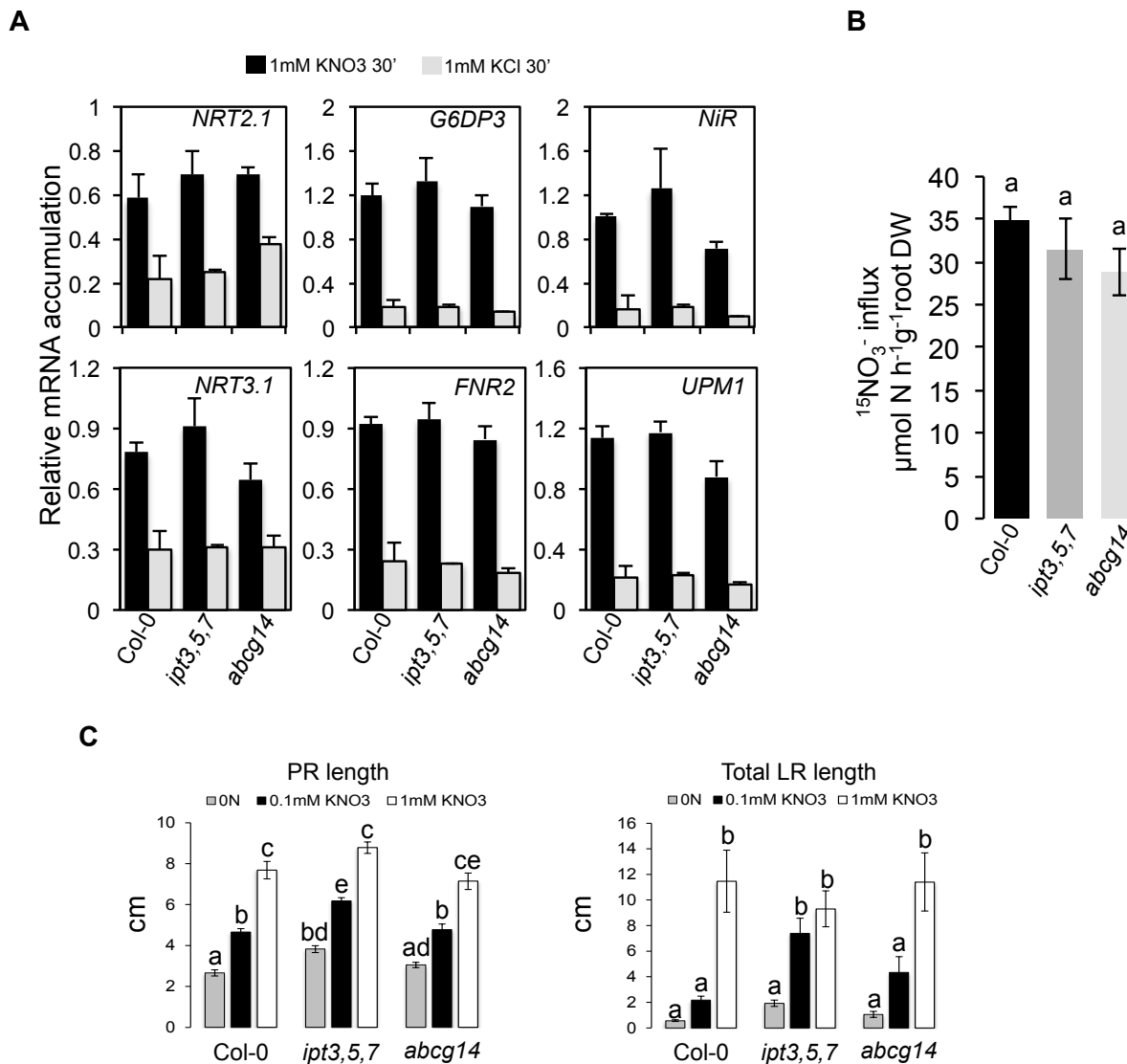
329
 330 **Figure 4. Responses of integrated traits to N-systemic signaling are affected in CK mutants.**
 331 (A) Individual root $^{15}\text{NO}_3^-$ influx is plotted against the root biomass. Root biomass and root $^{15}\text{NO}_3^-$ influx means are
 332 presented out of the graphs, below and on the left of each plot, respectively. On the left panel, the effects of N-
 333 demand systemic signaling in Col-0, *ipt3,5,7* and *abcg14* are shown by comparing C.KNO3 and Sp.KNO3 roots. On
 334 the right panel, effects of N-supply systemic signaling in Col-0, *ipt3,5,7* and *abcg14* are shown by comparing C.KCl
 335 and Sp.KCl roots. Graphs on top, middle and bottom correspond to Col-0, *ipt3,5,7* and *abcg14*, respectively. Data
 336 were obtained from 3 independent experiments, each including 6 biological replicates. Asterisks indicate significant
 337 differences between means, according to t-test with $p < 0.05^*$, $p < 0.01^{**}$, $p < 0.001^{***}$.
 338 (B) To generate the bar graph, we used root NO_3^- influx measurements from roots displaying dry weight below the
 339 arbitrary value of 2 mg, corresponding to 1/3 of the measurements presented in (A).
 340

341 **Local nitrate response is not impaired in cytokinin mutants.**

342
343 Previously, we have shown that root response to heterogeneous NO_3^- supply depends on a long-distance
344 signaling network triggered by NO_3^- *per se*. Indeed, the regulation of the specific and early sentinel genes
345 in heterogeneous conditions is similar between WT plants and NR-null mutant, leading to the conclusion
346 that the perception of NO_3^- is a prerequisite to trigger the response to systemic signaling (Ruffel et al.
347 2011). Thus, in order to rule out that the *ipt3,5,7* and *abcg14* mutants are impaired for their molecular and
348 physiological response to heterogeneous NO_3^- conditions only because they can not perceive local NO_3^-
349 provision, we evaluated their respective responsiveness to homogeneous NO_3^- supply. We first tested the
350 PNR (Medici and Krouk 2014) in the two mutants, by transferring plants from N free solution to 1 mM
351 KNO_3 or 1 mM KCl for 30 min. In the two mutants, the activation of NO_3^- -responsive marker genes was
352 similar to that observed in WT plants (Figure 5A). Although not significant, a reduction of NO_3^- induction
353 was observed for some nitrate-responsive marker genes in the *abcg14* mutant (e.g., *Nitrite Reductase-*
354 *NiR*). However, multiple biological replicates did not confirm that this mutant is impaired in NO_3^-
355 perception (Supplemental Figure 5). The capacity of *ipt3,5,7* and *abcg14* mutants to react to NO_3^- addition
356 was also supported by a similar root high affinity NO_3^- influx level between the 3 genotypes, at the same
357 time point selected to evaluate PNR (Figure 5B).

358 Similarly, the absence of root biomass changes in response to systemic signaling in the mutants
359 (Figure 4A) prompted us to verify that they are not only restrained in their capacity to grow,
360 independently of N supply conditions. When the three genotypes were grown on N-free, 0.1mM KNO_3 or
361 1mM KNO_3 containing media, the primary root length and total lateral root length increased with N
362 concentration for the 3 genotypes (Figure 5C), with a longer primary root in the *ipt3,5,7* mutant as
363 previously shown (Miyawaki et al. 2006). Thus, we confirmed that these mutants have the capacity to
364 grow with increasing N concentration.

365 Altogether, we conclude that CK biosynthesis and root-to-shoot translocation do not impair NO_3^-
366 perception as well as the potential to use N or to grow continuously in accordance with N supply but is
367 rather important to finely tune functional root response when N is partially or completely absent.



369

370 **Figure 5. Primary NO_3^- response and NO_3^- dependent root development are not impaired in CK mutants.**

371 (A) Relative expression level of 6 marker genes of the primary NO_3^- response *NRT2.1*, *NRT3.1*, *NiR*, *G6DP3*, *UPM1*
 372 and *FNR2* in roots from Col-0, *ipt3,5,7*, and *abcg14* plants transferred 30 min in media containing 1 mM KNO_3 (dark
 373 bars) or 1mM KCl (grey bars) as the control. Data are means (+/- SE) obtained from 2 independent experiments
 374 including in each 2 pools of 5-6 plants.

375 (B) Root $^{15}\text{NO}_3^-$ influx in 0.2 mM K^{15}NO_3 , in Col-0 (dark bar), *ipt3,5,7* (dark grey bar) and *abcg14* (light grey bar)
 376 plants prior exposed to KNO_3 1 mM for 30 min. Data are means (+/- SE) obtained from 24 individual plants from 2
 377 independent experiments. (C) Primary and lateral root length were measured in WT and mutant plants grown for 17
 378 days in N-free, KNO_3 0.1 mM or KNO_3 1mM containing medium. Data are means (+/-SE) determined from 6 to 12
 379 plants. Letters indicate significant difference according to a one-way analysis of variance followed by tukey post-hoc
 380 test; $p < 0.05$.

381 **DISCUSSION**

382
383 Functional root responses to N availability are the results of a complex signaling network integrating a
384 localized sensing of root NO_3^- availability with long-distance signaling aimed at coordinating the needs of
385 the different parts of the plant. Here, we show that the integration of *tZ* content in shoots is an essential
386 component of the long-distance signaling network controlling root responses. Our results, supported by
387 previous works focusing on the functional characterization of genes involved in CK biosynthesis
388 (Sakakibara et al. 2006; Kiba et al. 2013; Osugi et al. 2017), suggest that NO_3^- triggers *tZ* biosynthesis
389 mainly in roots. The *tZ*-types would be then transported to the shoots *via* ABCG14 where they modify
390 gene expression and possibly the associated metabolism. Therefore, our model would propose that NO_3^-
391 provision lead to *tZ* accumulation in roots that are subsequently transported to the shoots. The
392 accumulation of *tZ*, differing between homogeneous or heterogeneous conditions, would be integrated at
393 the shoot level leading to a differential control of root response according to NO_3^- provision applied to the
394 roots. In this scenario, *tZ* translocation could even constitute a part of the systemic signal it-self triggering
395 a shoot to root signal that still needs to be identified.

396 In shoots, glutamine biosynthesis is a semantic term significantly influenced by *tZ* accumulation
397 (Figure 3). Interestingly, amino acids have been hypothesized to be reporters of the N status of the plant
398 (Cooper and Clarkson 1989; Muller and Touraine 1992). We now hypothesize that CK-dependent NO_3^-
399 related signals could modify shoot glutamine or glutamate metabolism and that this might be part of a
400 branch of the shoot-to-root signal as previously hypothesized by others (Imsande and Touraine 1994; Gent
401 and Forde 2017; Girin et al. 2010). Of course, further studies will be necessary to validate this hypothesis,
402 but our work provides new experimental and genome-wide clues concerning the potential role of amino
403 acids as part of the shoot-to-root signaling.

404 We confirmed that CK accumulation is deeply affected in the *ipt3,5,7* and *abcg14* mutants (Figure
405 2) (Miyawaki et al. 2004; Ko et al. 2014; Zhang et al. 2014). Despite the strong repressive effect of local
406 CK status on root development (Werner et al. 2010; Laplaze et al. 2007), we have found that these
407 mutants, in particular *abcg14*, still maintain a certain capacity to adapt their development in particular to
408 homogenous N provision (Figure 5C). This could be explained by recent results obtained on CK
409 partitioning between the apoplasm and the cytosol. Indeed, an important aspect of CK signaling is that
410 CKs are perceived in the apoplasm and that the PUP14 transporter is crucial to import bioactive CKs into
411 the cytosol and suppress the CK response (Zürcher et al. 2016). In this perspective, we think that CK
412 accumulation is important but active CK transport at the cellular level in roots can, to some extent, explain
413 the responsiveness of *ipt3,5,7* and *abcg14* mutants.

414 Finally, this work refines the model of integration of the different N-related long-distance signaling
415 pathways displaying some differences with the CEP-related long distance model. Indeed, CEPs were
416 shown to be synthesized in N deprived roots and transported to the shoots where they are recognized by
417 their related receptor kinase (CEPR1) (Tabata et al. 2014). This recognition activates the biosynthesis of
418 CEPD1 polypeptides that are transported to the root where they activate *NRT2.1* transcript accumulation
419 (Ohkubo et al. 2017). Thus the CEP model is drastically triggered by N deprivation. In our model, we
420 believe that the long distance signal is generated by NO_3^- itself. Indeed, we observed that *tZ* accumulation
421 follows the NO_3^- provision level (Figure 2B). We thus hypothesize that the 2 models are likely relying on
422 different signaling modules. In nature, a plant shoot, experiencing root heterogeneous N conditions, likely
423 receives a combination of different long-distance signals coming from the different parts of the plant
424 (including CEP from N deprived roots and CK from NO_3^- supply roots). Future investigations will aim to
425 resolve how plants integrate in shoots these different signaling pathways to reach a coherent root adaptive
426 response.

427

428 MATERIALS AND METHODS

429

430 Plant materials

431 *Arabidopsis thaliana* Col-0 background was used as WT plant. The *abcg14* (SK_15918) mutant line was
432 kindly provided by Donghwi Ko (The Sainsbury Laboratory, Cambridge, UK). The *ipt3,5,7* triple mutant
433 line was previously kindly provided by Sabrina Sabatini (University “La Sapienza”, Rome).

434

435 Plant growth conditions

436 All plants were grown in short day light period (8h light 23°C/16h dark 21°C) at $260 \mu\text{mol.m}^{-2}.\text{s}^{-1}$
437 intensity. Split-root *in vitro* culture was done as previously described (Ruffel et al. 2011). Briefly, plants
438 were grown on solid (1% agar type A) N-free modified basal MS medium complemented with 0.5 mM
439 NH_4 -succinate and 0.1 mM KNO_3 as N sources. At day 10, the primary root was cut off below the second
440 lateral root, to obtain 2 new ‘primary roots’. At day 14, plants were transferred in 1 mM NH_4 -succinate
441 splitted-medium in order to separate the root system in two isolated parts. At day 18, plants were
442 transferred in new split plates containing: basal MS medium supplemented with 1 mM KNO_3 on one side
443 (Sp. KNO_3) and 1 mM KCl on the other side (Sp.KCl) or 1 mM KNO_3 on both side (C. KNO_3) or 1 mM
444 KCl on both side (C.KCl). Mini hydroponic *in vitro* culture (Phytatrays) was based on the same media
445 described above and a similar timing but it did not include any root pruning. For split-root in hydroponic
446 system, seeds were sown on upside down eppendorf taps with 1 mm whole filled by H_2O -agar 0.5%
447 solution and grown during 7 days on tap water. Then, seedlings were grown on nutritive solution

448 containing KH_2PO_4 1 mM; $\text{MgSO}_4 \cdot 7\text{H}_2\text{O}$ 1 mM; K_2SO_4 0.25 mM; $\text{CaCl}_2 \cdot 2\text{H}_2\text{O}$ 2.5 mM; Na-Fe-EDTA 0.1
449 mM; KCl 50 μM ; H_3BO_3 7.5 μM ; $\text{MnSO}_4 \cdot \text{H}_2\text{O}$ 1.25 μM ; $\text{ZnSO}_4 \cdot 7\text{H}_2\text{O}$ 0.25 μM ; $\text{CuSO}_4 \cdot 5\text{H}_2\text{O}$ 0.25 μM ;
450 $(\text{NH}_4)_6\text{Mo}_7\text{O}_{24} \cdot 4\text{H}_2\text{O}$ 0.025 μM ; supplied with 1 mM NH_4Cl and 0.1 mM KNO_3 as N sources, pH 5.8.
451 Nutritive solution was renewed every 4 days. 17 days after sowing, primary root was cut off below the
452 second lateral root, to obtain 2 root systems. After 4 additional days, plants were transferred in split root
453 system with 1 mM NH_4Cl as the sole N source for 4 more days to let the roots grow in split conditions.
454 24 hrs before treatment, nutrient solution is renewed by a N-free nutritive solution. Treatments are applied
455 by adding concentrated KNO_3 or KCl solution in each compartment up to a final concentration of 1 mM.
456 For PNR analysis, plants were grown exactly as we did for split-root experiments, except that the primary
457 root was not cut and thus the root system was not splitted in 2 parts at the time of the treatment. For root
458 development traits analysis, plants were sown and grown for 17 days *in vitro*, in square plates containing
459 modified N-free basal MS supplied with 0, 0.1 or 1 mM KNO_3 , 0.3 mM sucrose, 0.5 g/L MES and 1%
460 agar type A. Time collection or analysis of plants tissues was done as indicated in the results.

461

462 **Gene expression analysis**

463 Total RNA was extracted from frozen and grounded root or shoot tissues using TRIzolTM reagent
464 (15596026, ThermoFisher Scientific), following provider's instructions. RNA integrity and concentration
465 were determined using a 2100 Bioanalyzer Instrument (Agilent) and Agilent RNA 6000 Nano kit (5067-
466 1511, Agilent). DNA contamination was removed by digestion with DNase I (AMPD1, SIGMA). For
467 real-time qPCR analysis, reverse transcription of mRNAs was done using ThermoScriptTM RT-PCR
468 (11146016, ThermoFisher Scientific) according to the manufacturer's protocol. Gene expression was
469 determined using a LightCycler[®] 480 Instrument (Roche) and SYBR[®] Premix Ex TaqTM (RR420L,
470 TaKaRa). Expression levels of tested genes were normalized using the expression level of *Actin2/8* and
471 *Clathrin* genes. All specific primers used in this study are listed in Supplemental Table 3. Genome-wide
472 expression analysis in shoots was based on 4 biological replicates obtained from 4 independent
473 experiments including the 3 treatments (*i.e.*, C. KNO_3 , Split, C.KCl) and the 3 genotypes (*i.e.*, Col-0,
474 *ipt3,5,7*, *abcg14*). Gene expression measurements were performed using *Arabidopsis* Affymetrix[®]
475 Gene1.1 ST array strips designed to measure whole transcript accumulation of 28.501 genes (or transcripts
476 clusters), based on 600.941 probes defined on TAIR10 genome annotation. Biotin labeled and fragmented
477 cRNAs were obtained using GeneChip[®] WT PLUS Reagent kit (902280, ThermoFisher Scientific)
478 following manufacturer's instructions. Hybridization on array strips was performed for 16 hours at 48°C.
479 Arrays are washed, stained and scanned using GeneAtlas HWS Kit (901667, ThermoFisher Scientific) on
480 the GeneAtlas[®] Fluidics and Imaging Station.

481

482 **Statistical analysis and Bioinformatics**

483 Microarrays raw data were processed with GCRMA available on the Expression Console Software
484 developed by Affymetrix. Data analysis was performed in [R]. Genes differentially expressed specifically
485 in WT were identified by a t-test analysis (p-value<0.05). Genes responding to the treatment in 3
486 genotypes have been identified using a two-way ANOVA that was modeled as follows: $Y = \mu + \alpha_{\text{genotype}} +$
487 $\beta_{\text{treatment}} + (\alpha\beta)_{\text{genotype* treatment}} + \epsilon$, where Y is the normalized expression signal of a gene, μ is the global
488 mean, the α and β -coefficients correspond to the effects of NO_3^- availability (homogeneous or
489 heterogeneous), of the genotype and of the interaction between both factors, and ϵ represents unexplained
490 variance. All the genes for which at least the $\beta_{\text{treatment}}$ is significant (p-value<0.05) to explain variation of
491 expression have been selected. Hierarchical clustering of gene expression was performed using
492 MultiExperiment Viewer v4.8 (MeV) software (Saeed et al. 2003). Functional analysis of gene lists was
493 performed using the GeneCloud platform and semantic enrichment was displayed using word clouds
494 (<https://m2sb.org>) (Krouk et al. 2015).

495

496 **Determination of cytokinin content**

497 CK purification was performed according to the described method (Svačinová et al. 2012) with
498 modifications (Smehilova et al. 2016). Briefly, CKs were extracted from 30 mg of frozen powder in
499 modified Bielecki buffer (methanol/water/formic acid, 15/4/1, v/v/v) together with a cocktail of stable
500 isotope-labeled internal standards (0.25 pmol of CK bases, ribosides and N-glucosides, 0.5 pmol of CK O-
501 glucosides and nucleotides per sample added), and purified using two solid phase extraction columns. CK
502 content was determined by UHPLC–MS/MS (Ultra-High Performance Liquid Chromatography coupled to
503 a triple quadrupole mass spectrometer equipped with an electrospray interface). The quantification was
504 performed by Masslynx software (v4.1; Waters) using a standard isotope dilution method. The ratio of
505 endogenous CK to the appropriate labeled standard was determined and further used to quantify the level
506 of endogenous compounds in the original extract according to the known quantity of the added internal
507 standard.

508

509 **Determination of root biomass and nitrate influx capacity**

510 Root $^{15}\text{NO}_3^-$ influx was assayed as described previously (Munos et al. 2004). Root systems were rinsed
511 with 0.1 mM CaSO_4 solution for 1 min, transferred to nutrient solution containing 0.2 mM $^{15}\text{NO}_3^-$ (99%
512 atom excess ^{15}N) at pH 5.8, for 5 min and washed with 0.1 mM CaSO_4 solution for 1 min. Roots and the
513 shoots were harvested separately and dried in a oven at 70°C for 48 hrs. Dry weight was determined and
514 the total nitrogen and atom % ^{15}N were determined by continuous-flow isotope ratio mass spectrometer,

515 using a Euro-EA Euro Vector elemental analyzer coupled with an IsoPrime mass spectrometer (GV
516 Instruments).

517
518 **Measurements of root development traits**
519 Scans of the square plates containing the plants were performed at 600 dpi in TIFF format using a HP
520 scanner. Length of primary and lateral roots as well as the number of lateral roots were measured using
521 ImageJ software (Rasband 1997-2016).

522
523

524 **FUNDING**
525 This work was supported by Institut National de La Recherche Agronomique (CJS Fellowship to A.P. and
526 BAP project VARNET to S.R.), National Science Foundation (IOS 1339362-NutriNet with a fellowship
527 to A.C.) and Agence Nationale de la Recherche (IMANA ANR-14-CE19-0008). I.P. and O.N. were
528 supported by the Czech Science Foundation (project GA17-06613S) and the Ministry of Education, Youth
529 and Sport of the Czech Republic (National Program for Sustainability I, grant LO1204).

530
531 **AUTHOR CONTRIBUTIONS**
532 A.P., A.C., I.P. and O.N. performed research; A.P. and S.R. analyzed data. G.K., B.L. and S.R. designed
533 research and wrote the manuscript.

534
535 **ACKNOWLEDGEMENTS**
536 We thank Hugues Baudot and his team for taking care of the plant culture system, Pascal Tillard for ¹⁵N
537 measurements and Hana Martinková for her help with phytohormone analyses.

538
539 **REFERENCES**
540 Alvarez JM, Riveras E, Vidal EA, Gras DE, Contreras-Lopez O, Tamayo KP, Aceituno F, Gomez I,
541 Ruffel S, Lejay L, Jordana X, Gutierrez RA (2014) Systems approach identifies TGA1 and TGA4
542 transcription factors as important regulatory components of the nitrate response of Arabidopsis
543 thaliana roots. *Plant J* 80 (1):1-13.
544 Alvarez JM, Vidal EA, Gutierrez RA (2012) Integration of local and systemic signaling pathways for
545 plant N responses. *Curr Opin Plant Biol* 15 (2):185-191.
546 Araus V, Vidal EA, Puelma T, Alamos S, Mieulet D, Guiderdoni E, Gutierrez RA (2016) Members of
547 BTB Gene Family of Scaffold Proteins Suppress Nitrate Uptake and Nitrogen Use Efficiency.
548 *Plant Physiol* 171 (2):1523-1532.
549 Araya T, Miyamoto M, Wibowo J, Suzuki A, Kojima S, Tsuchiya YN, Sawa S, Fukuda H, von Wiren N,
550 Takahashi H (2014) CLE-CLAVATA1 peptide-receptor signaling module regulates the expansion
551 of plant root systems in a nitrogen-dependent manner. *Proc Natl Acad Sci USA* 111 (5):2029-
552 2034.

553 Bishopp A, Lynch JP (2015) The hidden half of crop yields. *Nat Plants* 1:15117.
554 Castaings L, Camargo A, Pocholle D, Gaudon V, Texier Y, Boutet-Mercey S, Taconnat L, Renou JP,
555 Daniel-Vedele F, Fernandez E, Meyer C, Krapp A (2009) The nodule inception-like protein 7
556 modulates nitrate sensing and metabolism in Arabidopsis. *Plant J* 57 (3):426-435.
557 Cooper HD, Clarkson DT (1989) Cycling of amino-nitrogen and other nutrient between shoots and roots
558 in cereals: a possible mechanism integrating shoot and root in the regulation of nutrient uptake. *J*
559 *Exp Bot* 40:753-762.
560 Den Herder G, Van Isterdael G, Beeckman T, De Smet I (2010) The roots of a new green revolution.
561 *Trends Plant Sci* 15 (11):600-607.
562 Filleur S, Dorbe MF, Cerezo M, Orsel M, Granier F, Gojon A, Daniel-Vedele F (2001) An arabidopsis T-
563 DNA mutant affected in Nrt2 genes is impaired in nitrate uptake. *FEBS Lett* 489 (2-3):220-224.
564 Forde B (2014) Nitrogen signalling pathways shaping root system architecture: an update. *Curr Opin Plant*
565 *Biol* 21:30-36.
566 Gansel X, Munos S, Tillard P, Gojon A (2001) Differential regulation of the NO₃- and NH₄⁺ transporter
567 genes AtNrt2.1 and AtAmt1.1 in Arabidopsis: relation with long-distance and local controls by N
568 status of the plant. *Plant J* 26 (2):143-155.
569 Gent L, Forde BG (2017) How do plants sense their nitrogen status? *J Exp Bot* 68 (10):2531-2539.
570 Gifford ML, Dean A, Gutierrez RA, Coruzzi GM, Birnbaum KD (2008) Cell-specific nitrogen responses
571 mediate developmental plasticity. *Proc Natl Acad Sci U S A* 105 (2):803-808.
572 Girin T, El-Kafafi el S, Widiez T, Erban A, Hubberten HM, Kopka J, Hoefgen R, Gojon A, Lepetit M
573 (2010) Identification of Arabidopsis mutants impaired in the systemic regulation of root nitrate
574 uptake by the nitrogen status of the plant. *Plant Physiol* 153 (3):1250-1260.
575 Gruber BD, Giehl RF, Friedel S, von Wiren N (2013) Plasticity of the Arabidopsis root system under
576 nutrient deficiencies. *Plant Physiol* 163 (1):161-179.
577 Guan P, Ripoll J-J, Wang R, Vuong L, Bailey-Steinitz LJ, Ye D, Crawford NM (2017) Interacting TCP
578 and NLP transcription factors control plant responses to nitrate availability. *Proc Natl Acad Sci*
579 *USA* 114 (9):2419-2424.
580 Guan P, Wang R, Nacry P, Breton G, Kay SA, Pruneda-Paz JL, Davani A, Crawford NM (2014) Nitrate
581 foraging by Arabidopsis roots is mediated by the transcription factor TCP20 through the systemic
582 signaling pathway. *Proc Natl Acad Sci USA* 111 (42):15267-15272.
583 Gutierrez RA, Stokes TL, Thum K, Xu X, Obertello M, Katari MS, Tanurdzic M, Dean A, Nero DC,
584 McClung CR, Coruzzi GM (2008) Systems approach identifies an organic nitrogen-responsive
585 gene network that is regulated by the master clock control gene CCA1. *Proc Natl Acad Sci USA*
586 105 (12):4939-4944.
587 Ho CH, Lin SH, Hu HC, Tsay YF (2009) CHL1 functions as a nitrate sensor in plants. *Cell* 138 (6):1184-
588 1194.
589 Hu HC, Wang YY, Tsay YF (2009) AtCIPK8, a CBL-interacting protein kinase, regulates the low-affinity
590 phase of the primary nitrate response. *Plant J* 57 (2):264-278.
591 Imsande J, Touraine B (1994) N demand and the regulation of nitrate uptake. *Plant Physiol* 105:3-7.
592 Kellermeier F, Armengaud P, Seditas TJ, Danku J, Salt DE, Amtmann A (2014) Analysis of the Root
593 System Architecture of Arabidopsis Provides a Quantitative Readout of Crosstalk between
594 Nutritional Signals. *Plant Cell* 26 (4):1480-1496.
595 Kiba T, Takei K, Kojima M, Sakakibara H (2013) Side-chain modification of cytokinins controls shoot
596 growth in Arabidopsis. *Developmental cell* 27 (4):452-461.
597 Ko D, Kang J, Kiba T, Park J, Kojima M, Do J, Kim KY, Kwon M, Endler A, Song WY, Martinoia E,
598 Sakakibara H, Lee Y (2014) Arabidopsis ABCG14 is essential for the root-to-shoot translocation
599 of cytokinin. *Proc Natl Acad Sci USA* 111 (19):7150-7155.
600 Kong X, Zhang M, De Smet I, Ding Z (2014) Designer crops: optimal root system architecture for nutrient
601 acquisition. *Trends Biotechnol* 32 (12):597-598.
602 Konishi M, Yanagisawa S (2013) Arabidopsis NIN-like transcription factors have a central role in nitrate
603 signalling. *Nat Comm* 4:1617.

604 Krouk G (2017) Nitrate signalling: Calcium bridges the nitrate gap. *Nat Plants* 3:17095.

605 Krouk G, Carré C, Fizames C, Gojon A, Ruffel S, Lacombe B (2015) GeneCloud Reveals Semantic
606 Enrichment in Lists of Gene Descriptions. *Mol Plant* 8 (6):971-973.

607 Krouk G, Lacombe B, Bielach A, Perrine-Walker F, Malinska K, Mounier E, Hoyerova K, Tillard P, Leon
608 S, Ljung K, Zazimalova E, Benkova E, Nacry P, Gojon A (2010a) Nitrate-regulated auxin
609 transport by NRT1.1 defines a mechanism for nutrient sensing in plants. *Dev Cell* 18 (6):927-937.

610 Krouk G, Mirowski P, LeCun Y, Shasha DE, Coruzzi GM (2010b) Predictive network modeling of the
611 high-resolution dynamic plant transcriptome in response to nitrate. *Genome Biol* 11 (12):R123.

612 Krouk G, Ruffel S, Gutierrez RA, Gojon A, Crawford NM, Coruzzi GM, Lacombe B (2011) A framework
613 integrating plant growth with hormones and nutrients. *Trends Plant Sci* 16 (4):178-182.

614 Laplaze L, Benkova E, Casimiro I, Maes L, Vanneste S, Swarup R, Weijers D, Calvo V, Parizot B,
615 Herrera-Rodriguez MB, Offringa R, Graham N, Doumas P, Friml J, Bogusz D, Beeckman T,
616 Bennett M (2007) Cytokinins act directly on lateral root founder cells to inhibit root initiation.
617 *Plant Cell* 19 (12):3889-3900.

618 Lérans S, Edel KH, Pervent M, Hashimoto K, Corratgé-Faillie C, Offenborn JN, Tillard P, Gojon A, Kudla
619 J, Lacombe B (2015) Nitrate sensing and uptake in *Arabidopsis* are enhanced by ABI2, a
620 phosphatase inactivated by the stress hormone abscisic acid. *Sci Signal* 8 (375):ra43.

621 Li C, Potuschak T, Colon-Carmona A, Gutierrez RA, Doerner P (2005) *Arabidopsis* TCP20 links
622 regulation of growth and cell division control pathways. *Proc Natl Acad Sci USA* 102 (36):12978-
623 12983.

624 Li Y, Krouk G, Coruzzi GM, Ruffel S (2014) Finding a nitrogen niche: a systems integration of local and
625 systemic nitrogen signalling in plants. *J Exp Bot* 65 (19):5601-5610.

626 Liu K-h, Niu Y, Konishi M, Wu Y, Du H, Sun Chung H, Li L, Boudsocq M, McCormack M, Maekawa S,
627 Ishida T, Zhang C, Shokat K, Yanagisawa S, Sheen J (2017) Discovery of nitrate-CPK-NLP
628 signalling in central nutrient-growth networks. *Nature* 545 (7654):311-316.

629 Marchive C, Roudier F, Castaigns L, Brehaut V, Blondet E, Colot V, Meyer C, Krapp A (2013) Nuclear
630 retention of the transcription factor NLP7 orchestrates the early response to nitrate in plants. *Nat*
631 *Comm* 4:1713.

632 Medici A, Krouk G (2014) The primary nitrate response: a multifaceted signalling pathway. *J Exp Bot* 65
633 (19):5567-5576.

634 Miyawaki K, Matsumoto-Kitano M, Kakimoto T (2004) Expression of cytokinin biosynthetic
635 isopentenyltransferase genes in *Arabidopsis*: tissue specificity and regulation by auxin, cytokinin,
636 and nitrate. *Plant J* 37 (1):128-138.

637 Miyawaki K, Tarkowski P, Matsumoto-Kitano M, Kato T, Sato S, Tarkowska D, Tabata S, Sandberg G,
638 Kakimoto T (2006) Roles of *Arabidopsis* ATP/ADP isopentenyltransferases and tRNA
639 isopentenyltransferases in cytokinin biosynthesis. *Proc Natl Acad Sci USA* 103 (44):16598-
640 16603.

641 Mounier E, Pervent M, Ljung K, Gojon A, Nacry P (2014) Auxin-mediated nitrate signalling by NRT1.1
642 participates in the adaptive response of *Arabidopsis* root architecture to the spatial heterogeneity
643 of nitrate availability. *Plant Cell Environ* 37 (1):162-174.

644 Muller B, Touraine B (1992) Inhibition of NO₃- Uptake by Various Phloem-Translocated Amino Acids in
645 Soybean Seedlings. *J Exp Bot* 43 (5):617-623.

646 Munos S, Cazes C, Fizames C, Gaymard F, Tillard P, Lepetit M, Lejay L, Gojon A (2004) Transcript
647 profiling in the *chl1-5* mutant of *Arabidopsis* reveals a role of the nitrate transporter NRT1.1 in
648 the regulation of another nitrate transporter, NRT2.1. *Plant Cell* 16 (9):2433-2447.

649 O'Brien JA, Vega A, Bouguyon E, Krouk G, Gojon A, Coruzzi G, Gutierrez RA (2016) Nitrate Transport,
650 Sensing, and Responses in Plants. *Mol Plant* 9 (6):837-856.

651 Ohkubo Y, Tanaka M, Tabata R, Ogawa-Ohnishi M, Matsubayashi Y (2017) Shoot-to-root mobile
652 polypeptides involved in systemic regulation of nitrogen acquisition. *Nat Plants* 3:17029.

653 Osugi A, Kojima M, Takebayashi Y, Ueda N, Kiba T, Sakakibara H (2017) Systemic transport of trans-
654 zeatin and its precursor have differing roles in *Arabidopsis* shoots. *Nat Plants* 3:17112.

655 Rasband WS (1997-2016) ImageJ, U. S. National Institutes of Health, Bethesda, Maryland, USA,
656 <https://imagej.nih.gov/ij/>.

657 Remans T, Nacry P, Pervert M, Filleur S, Diatloff E, Mounier E, Tillard P, Forde BG, Gojon A (2006)
658 The Arabidopsis NRT1.1 transporter participates in the signaling pathway triggering root
659 colonization of nitrate-rich patches. *Proc Natl Acad Sci USA* 103 (50):19206-19211.

660 Riveras E, Alvarez JM, Vidal EA, Oses C, Vega A, Gutierrez RA (2015) The Calcium Ion Is a Second
661 Messenger in the Nitrate Signaling Pathway of Arabidopsis. *Plant Physiol* 169 (2):1397-1404.

662 Rubin G, Tohge T, Matsuda F, Saito K, Scheible WR (2009) Members of the LBD family of transcription
663 factors repress anthocyanin synthesis and affect additional nitrogen responses in Arabidopsis.
664 *Plant Cell* 21 (11):3567-3584.

665 Ruffel S, Freixes S, Balzergue S, Tillard P, Jeudy C, Martin-Magniette ML, van der Merwe MJ, Kakar K,
666 Gouzy J, Fernie AR, Udvardi M, Salon C, Gojon A, Lepetit M (2008) Systemic signaling of the
667 plant nitrogen status triggers specific transcriptome responses depending on the nitrogen source in
668 *Medicago truncatula*. *Plant Physiol* 146 (4):2020-2035.

669 Ruffel S, Gojon A (2017) Systemic nutrient signalling: On the road for nitrate. *Nat Plants* 3:17040.

670 Ruffel S, Krouk G, Ristova D, Shasha D, Birnbaum KD, Coruzzi GM (2011) Nitrogen economics of root
671 foraging: transitive closure of the nitrate-cytokinin relay and distinct systemic signaling for N
672 supply vs. demand. *Proc Natl Acad Sci USA* 108 (45):18524-18529.

673 Ruffel S, Poitout A, Krouk G, Coruzzi GM, Lacombe B (2016) Long-distance nitrate signaling displays
674 cytokinin dependent and independent branches. *J Integr Plant Biol* 58 (3):226-229.

675 Saeed AI, Sharov V, White J, Li J, Liang W, Bhagabati N, Braisted J, Klapa M, Currier T, Thiagarajan M,
676 Sturn A, Snuffin M, Rezantsev A, Popov D, Ryltsov A, Kostukovich E, Borisovsky I, Liu Z,
677 Vinsavich A, Trush V, Quackenbush J (2003) TM4: a free, open-source system for microarray
678 data management and analysis. *Biotechniques* 34 (2):374-378

679 Sakakibara H, Takei K, Hirose N (2006) Interactions between nitrogen and cytokinin in the regulation of
680 metabolism and development. *Trends Plant Sci* 11 (9):440-448.

681 Schafer M, Brutting C, Meza-Canales ID, Grosskinsky DK, Vankova R, Baldwin IT, Meldau S (2015)
682 The role of cis-zeatin-type cytokinins in plant growth regulation and mediating responses to
683 environmental interactions. *J Exp Bot* 66 (16):4873-4884.

684 Smehilova M, Dobruskova J, Novak O, Takac T, Galuszka P (2016) Cytokinin-Specific
685 Glycosyltransferases Possess Different Roles in Cytokinin Homeostasis Maintenance. *Front Plant*
686 *Sci* 7:1264.

687 Svačinová J, Novak O, Plačková L, Lenobel R, Holík J, Strnad M, Doležal K (2012) A new approach for
688 cytokinin isolation from Arabidopsis tissues using miniaturized purification: pipette tip solid-
689 phase extraction. *Plant Meth* 8 (17):1-14.

690 Tabata R, Sumida K, Yoshii T, Ohyama K, Shinohara H, Matsubayashi Y (2014) Perception of root-
691 derived peptides by shoot LRR-RKs mediates systemic N-demand signaling. *Science* 346
692 (6207):343-346.

693 Takei K, Sakakibara H, Taniguchi M, Sugiyama T (2001) Nitrogen-dependent accumulation of cytokinins
694 in root and the translocation to leaf: implication of cytokinin species that induces gene expression
695 of maize response regulator. *Plant Cell Physiol* 42 (1):85-93.

696 Takei K, Ueda N, Aoki K, Kuromori T, Hirayama T, Shinozaki K, Yamaya T, Sakakibara H (2004)
697 AtIPT3 is a Key Determinant of Nitrate-Dependent Cytokinin Biosynthesis in Arabidopsis. *Plant*
698 *Cell Physiol* 45 (8):1053-1062.

699 Vidal EA, Moyano TC, Riveras E, Contreras-Lopez O, Gutierrez RA (2013) Systems approaches map
700 regulatory networks downstream of the auxin receptor AFB3 in the nitrate response of
701 Arabidopsis thaliana roots. *Proc Natl Acad Sci USA* 110 (31):12840-12845.

702 Walch-Liu P, Filleur S, Gan Y, Forde BG (2005) Signaling mechanisms integrating root and shoot
703 responses to changes in the nitrogen supply. *Photosynth Res* 83 (2):239-250.

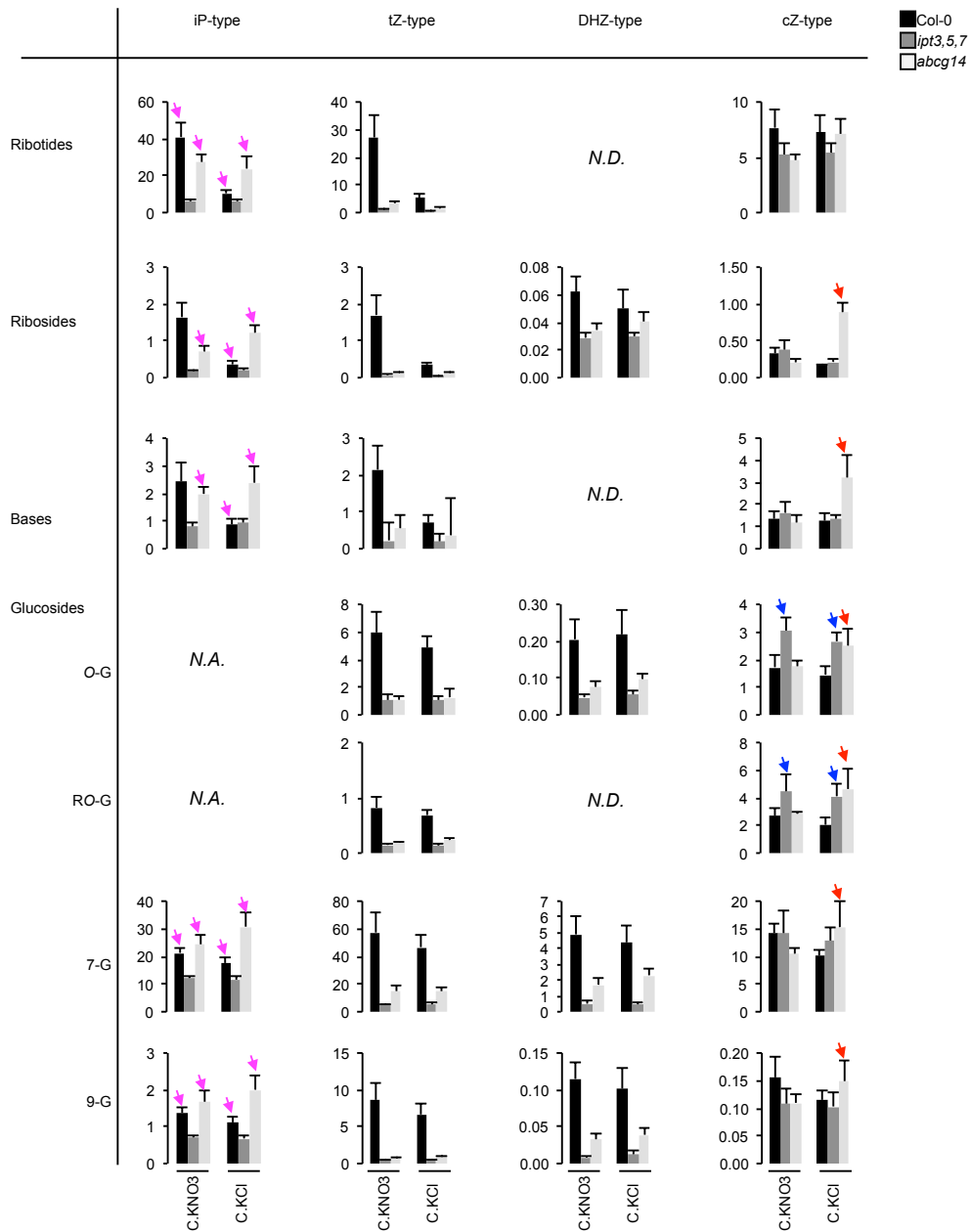
704 Werner T, Nehnevajova E, Kollmer I, Novak O, Strnad M, Kramer U, Schmulling T (2010) Root-specific
705 reduction of cytokinin causes enhanced root growth, drought tolerance, and leaf mineral
706 enrichment in Arabidopsis and tobacco. *Plant Cell* 22 (12):3905-3920.
707 Xu N, Wang R, Zhao L, Zhang C, Li Z, Lei Z, Liu F, Guan P, Chu Z, Crawford NM, Wang Y (2016) The
708 Arabidopsis NRG2 Protein Mediates Nitrate Signaling and Interacts with and Regulates Key
709 Nitrate Regulators. *Plant Cell* 28 (2):485-504.
710 Yong Z, Kotur Z, Glass AD (2010) Characterization of an intact two-component high-affinity nitrate
711 transporter from Arabidopsis roots. *Plant J* 63 (5):739-748.
712 Zhang H, Forde BG (1998) An Arabidopsis MADS Box Gene That Controls Nutrient-Induced Changes in
713 Root Architecture. *Science* 279 (5349):407-409.
714 Zhang K, Novak O, Wei Z, Gou M, Zhang X, Yu Y, Yang H, Cai Y, Strnad M, Liu CJ (2014) Arabidopsis
715 ABCG14 protein controls the acropetal translocation of root-synthesized cytokinins. *Nat Comm*
716 5:3274.
717 Zürcher E, Liu J, di Donato M, Geisler M, Müller B (2016) Plant development regulated by cytokinin
718 sinks. *Science* 353 (6303):1027-1030.
719

720 **Supplemental Information**

721 1. Supplemental Figures 1 to 5

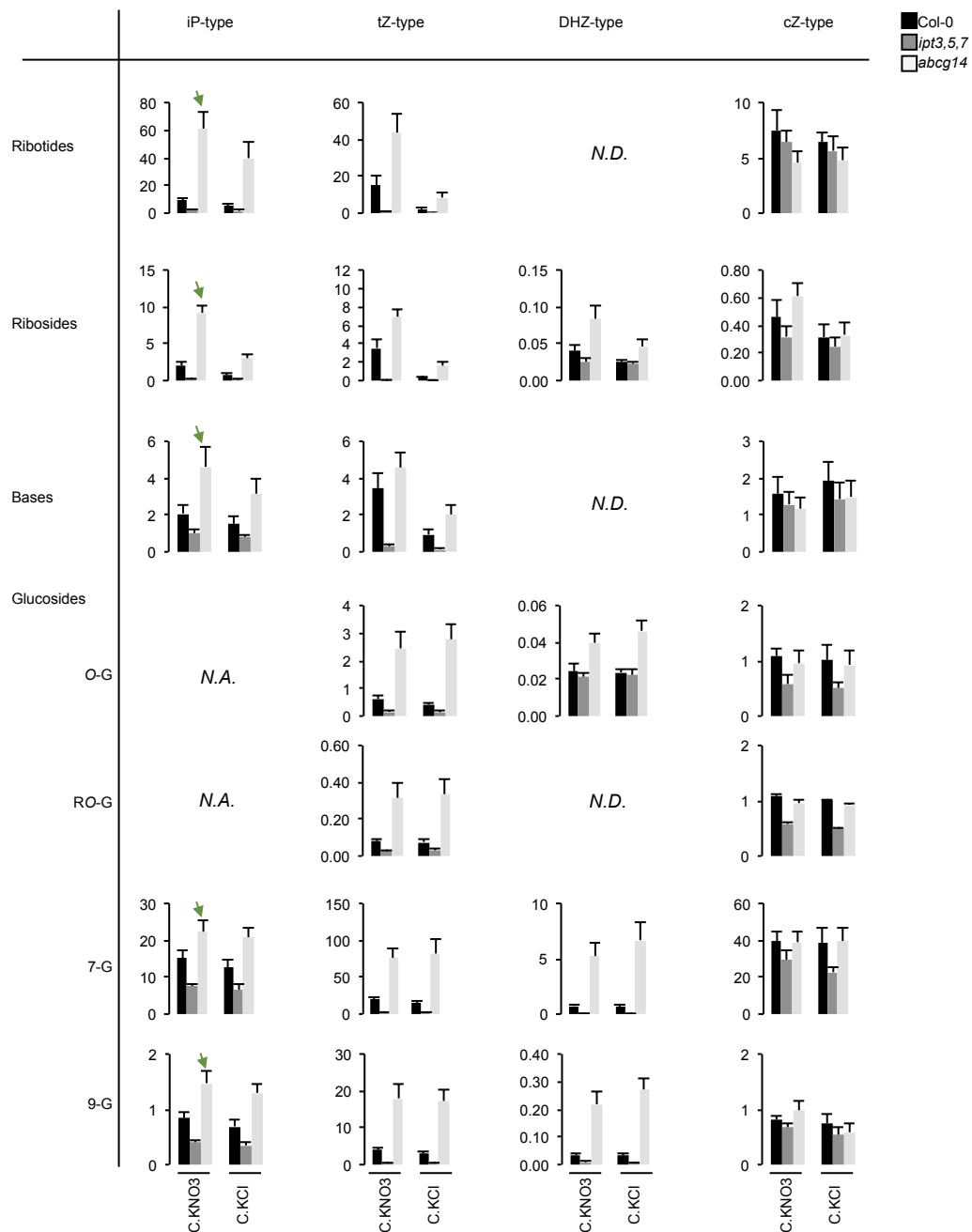
722 2. Supplemental Tables 1 to 3 (uploaded in separate files).

723



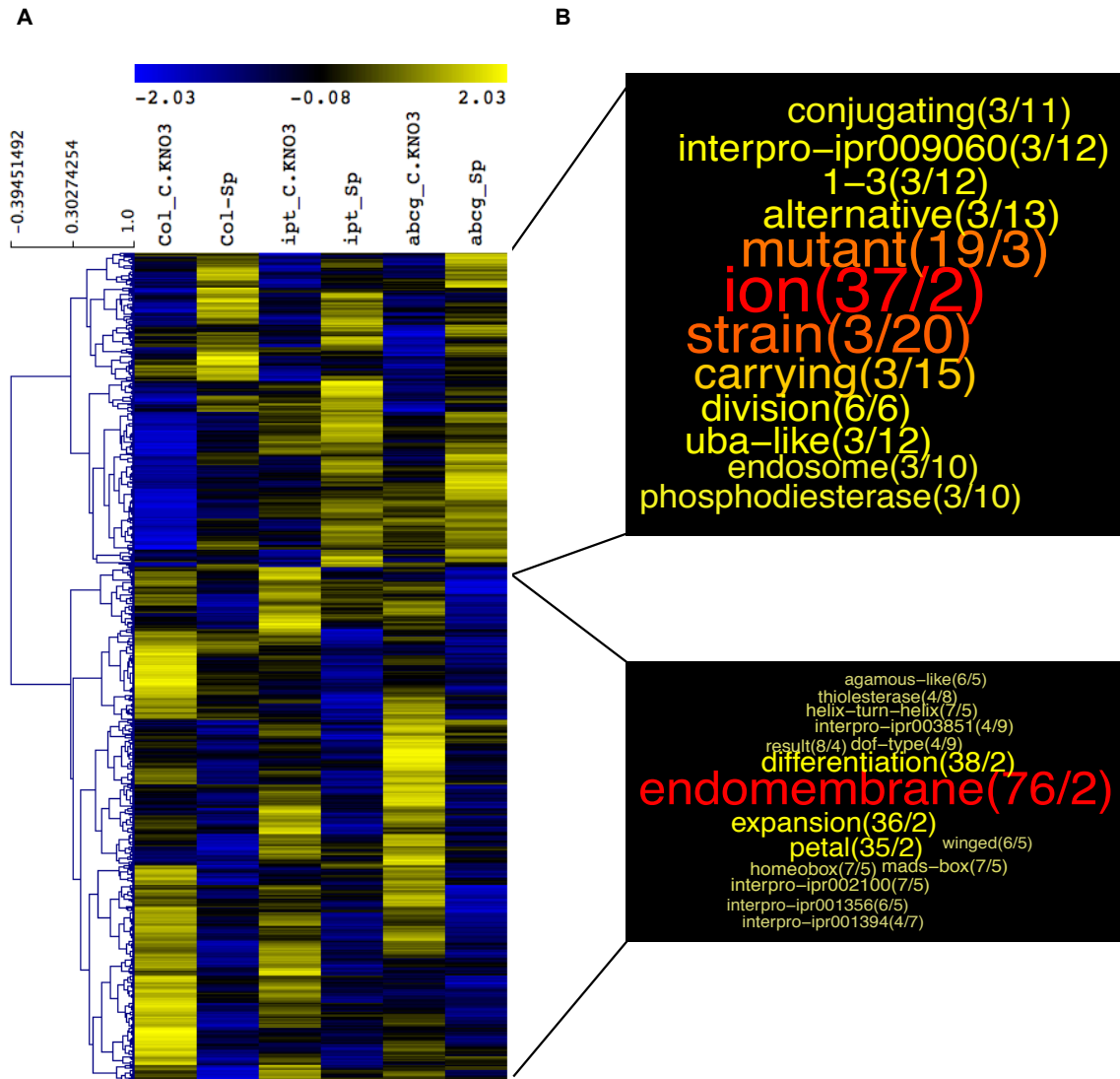
724
 725 **Supplemental Figure 1. CK contents in shoots of WT, *ipt3,5,7*, and *abcg14* plants exposed to split-**
 726 **root conditions.**

727 Barplots show total shoot accumulation of *tZ*, *iP*, *cZ* and DHZ-type CK respectively from left to right and
 728 ribotides, ribosides, bases and glucosides forms respectively from top to bottom. Black bars: WT; dark
 729 grey bars: *ipt3,5,7*; light grey bars: *abcg14*. Values are the means (+/- SE) of 5 to 6 biological replicates
 730 collected from 4 independent experiments. N.D.: Not Detected. N.A.: Not Applicable. *iP*: N^6 -(Δ^2 -
 731 isopentyl)adenine; *tZ*: *trans*-Zeatin; *cZ*: *cis*-Zeatin; DHZ: Dihydrozeatin. Pink arrows indicate that N-
 732 dependent *iP* accumulation is affected in *abcg14* compared to Col-0. Blue arrows indicate an increase of
 733 *O*-glucosylated *cZ* in *ipt3,5,7*. Red arrows indicate increase of *cZ* in *abcg14* in N-deprived conditions.



734
 735 **Supplemental Figure 2. CK contents in roots of WT, *ipt3,5,7*, and *abcg14* plants exposed to C.KNO3**
 736 **or C.KCl conditions.**

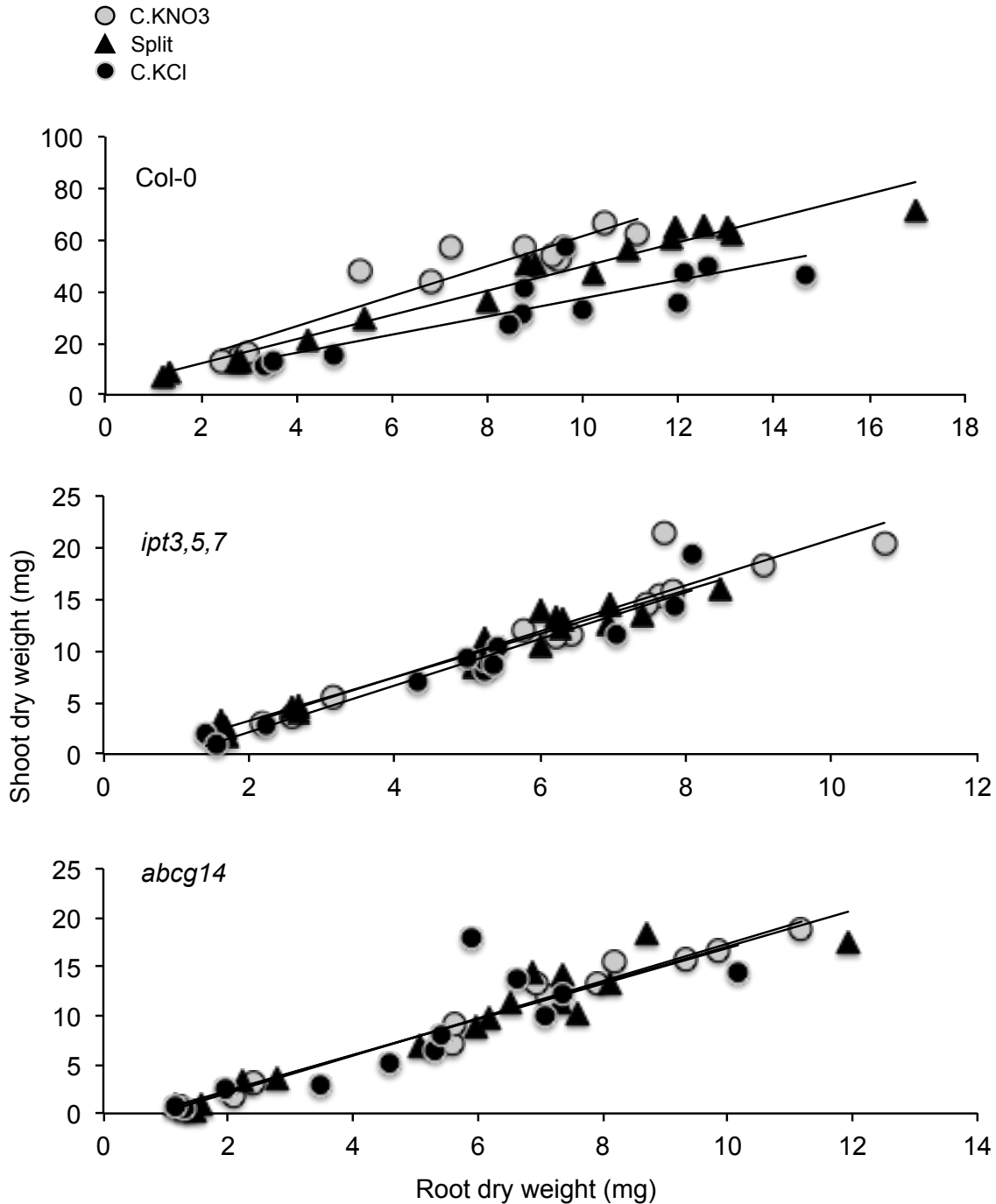
737 Barplots show total root accumulation of *tZ*, *iP*, *cZ* and *DHZ*-type CK respectively from left to right and
 738 ribotides, ribosides, bases and glucosides forms respectively from top to bottom. Black bars: WT; dark
 739 grey bars: *ipt3,5,7*; light grey bars: *abcg14*. Values are the means (+/- SE) of 5 to 6 biological replicates
 740 collected from 4 independent experiments. N.D.: Not Detected. N.A.: Not Applicable. *iP*: N^6 -(Δ^2 -
 741 isopentyl)adenine; *tZ*: *trans*-Zeatin; *cZ*: *cis*-Zeatin; *DHZ*: Dihydrozeatin. Green arrows indicate N-
 742 dependent *iP* accumulation in *abcg14* mutant.



743
 744 **Supplemental Figure 3. CK-independent shoot transcriptome changes in response to root**
 745 **heterogeneous NO₃⁻ supply.**

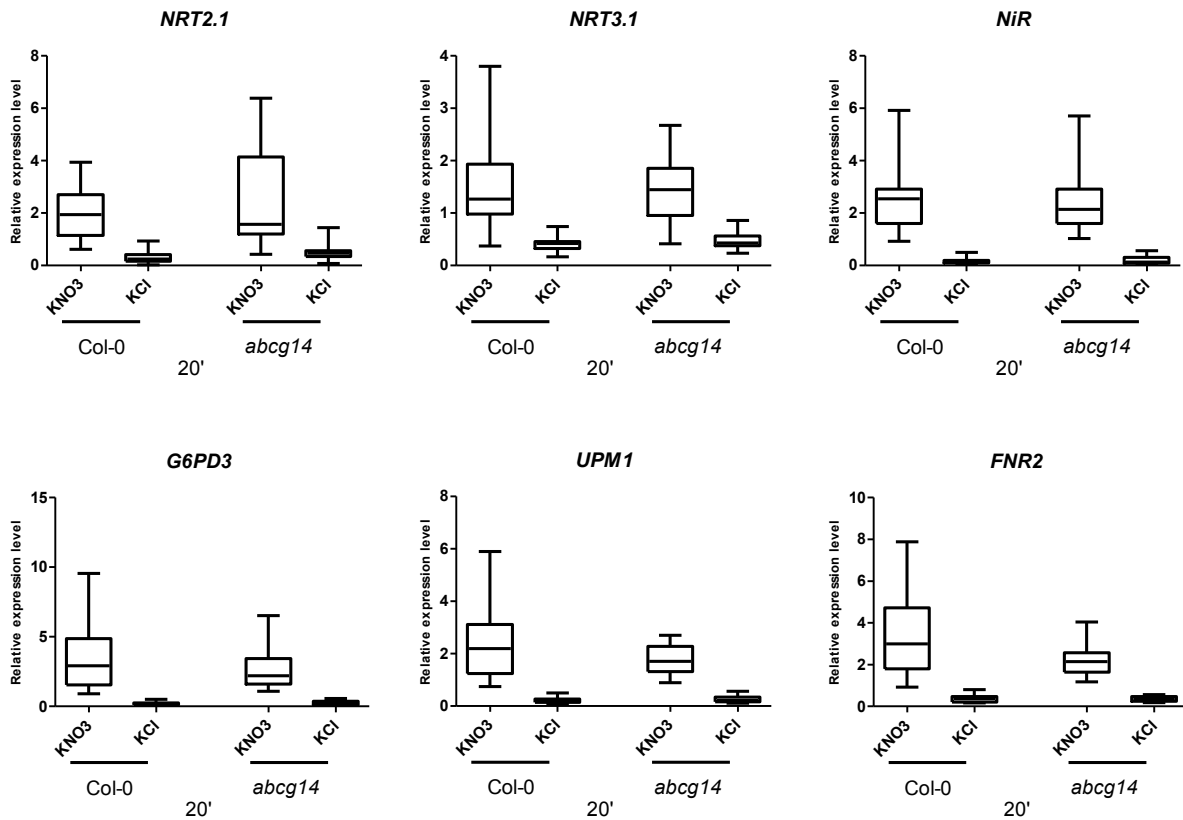
746 (A) Shoots of Col-0, *ipt3*, *ipt5*, *ipt7* and *abcg14* plants transferred for 24 hrs in NO₃⁻ homogeneous (C.KNO3) or
 747 heterogeneous (Split) environment were harvested for transcriptomic analysis. Samples of 4 biological
 748 replicates from 4 independent experiments were used to perform the microarray analysis, using
 749 Arabidopsis Gene1.1 ST array Strip (Affymetrix GeneAtlasTM). Hierarchical clustering of the 669 genes
 750 identified as differentially expressed in C.KNO3 versus Split conditions in the 3 genotypes was performed
 751 with Multiple Experiment Viewer (MeV) software (<http://mev.tm4.org/>).

752 (B) Semantic enrichment in annotation of genes induced (at the top) or repressed (bottom) in Split
 753 condition compared to C.KNO3 in WT shoots, based on a GeneCloud analysis (<https://m2sb.org>). Beside
 754 each term, the first number corresponds to the number of genes containing the term and the second
 755 number gives the fold enrichment.



756
 757 **Supplemental Figure 4. Dynamic of shoot/root ratio in response to N availability is lost in *ipt3,5,7***
 758 **and *abcg14* plants.**

759 Plots display relationship between root and shoot dry biomass from plants treated 4 days in NO₃⁻
 760 homogeneous (C.KNO3, grey circles), NO₃⁻ heterogeneous (Split, dark triangles) or N-deprived (C.KCl,
 761 dark circles) conditions in the WT, *ipt3,5,7* and *abcg14* mutants. Measurements result from 3 independent
 762 experiments. In each experiment, 6 biological replicates by conditions were measured.



763
 764 **Supplemental Figure 5. The ability of *abcg14* to trigger the primary NO₃⁻ response is confirmed in**
 765 **younger plants grown in mini hydroponic system.**

766 Boxplots display relative expression level of the 6 marker genes of the primary NO₃⁻ response: *NRT2.1*,
 767 *NRT3.1*, *NiR*, *G6PD3*, *UPM1* and *FNR2*, in roots of Col-0 and *abcg14*, 20 minutes after transferring the
 768 plants in 1 mM KNO₃ or 1 mM KCl containing medium. Data are means (+/-SE) obtained from 4
 769 independent experiments, including in each 2 or 3 biological replicates that correspond to a pool of 20 to
 770 50 plantlets.

771